Clays and Clay Minerals, Vol. 37, No. 2, 135–142, 1989.

AQUEOUS-CHEMICAL CONTROL OF THE TETRAHEDRAL-ALUMINUM CONTENT OF QUARTZ, HALLOYSITE, AND OTHER LOW-TEMPERATURE SILICATES

ENRIQUE MERINO, COLIN HARVEY,[1] AND H. H. MURRAY
Department of Geology, Indiana University, Bloomington, Indiana 47405

Abstract—Aqueous Al passes from octahedral to tetrahedral coordination over a narrow pH interval, or threshold. This interval is 5.5–6.5 at 25°C and shifts to lower pH as temperature increases. The concentration of aqueous tetrahedrally coordinated Al is a quasi-step function of the solution pH, and, by the mass-action law, so should be the amount of tetrahedral Al incorporated by a silicate that crystallizes from the aqueous solution. Qualitative support for this prediction (which applies to quartz, opal-CT, kaolin-group minerals, pyrophyllite, micas, chlorites, and other low-temperature silicates) comes from the very topology of equilibrium activity diagrams and from several pairs of associated waters and authigenic silicates from weathering, hydrothermal, and diagenetic environments. The uptake of tetrahedral Al also depends on the aqueous concentrations of monovalent cations and silica, and on the mineral's structural constraints.

Solid solution of tetrahedral Al in halloysite in turn produces the characteristic bent or tubular crystals of this mineral. This genetic link between aqueous chemistry (mainly pH), tetrahedral-Al uptake by a low-temperature silicate, and the mineral's crystal morphology may operate also in other silicates.

Key Words—Activity diagram, Al solid solution, Crystal morphology, Halloysite, Quartz, Step function, Water-silicate equilibria.

INTRODUCTION

Because of the mass-action law any mineral is forced to incorporate ions and species that are sufficiently concentrated in the aqueous solution from which it precipitates—although only to the degree allowed by its crystal structure. This general idea can explain why and under what conditions many silicates incorporate some tetrahedral Al in substitution for Si. Qualitatively, they do so if they crystallize from aqueous solutions having sufficiently high concentrations of *tetrahedral* Al. A similar suggestion was made in passing by de Jong *et al.* (1983).

The purpose of this contribution is to assess the consequences of aqueous-solution composition on the degree of uptake of tetrahedral Al by low-temperature silicates that crystallize from aqueous solution, and to test these predictions by comparing natural water compositions and associated authigenic silicates on activity diagrams. To simplify these comparisons we have taken aqueous-species activity coefficients to be similar to each other and thus to cancel out of mass-action law expressions; this assumption introduces at worst only second-order errors. Tetrahedrally coordinated and octahedrally coordinated Al are represented by Al^t and Al^o. The minerals considered below with regard to their ability to incorporate Al^t are quartz and halloysite, which exemplify a behavior probably displayed by kaolinite, pyrophyllite, micas, chlorites, and sepiolite as well. The thermodynamic data used below are, except where otherwise specified, from May *et al.* (1979), Coutourier *et al.* (1984), and Bowers *et al.* (1984).

COORDINATION OF ALUMINUM IN AQUEOUS SOLUTIONS

At low pHs the dominant species of Al in aqueous solutions is $[Al(H_2O)_6]^{3+}$, in which the Al ion is coordinated octahedrally by six water dipoles (Cotton and Wilkinson, 1962, pp. 335, 340; Hem and Robertson, 1967, p. A10). As the pH increases some of the dipoles lose a hydrogen ion, and the resulting hydroxyl ions are thus attracted more strongly by the inner Al ion. This attraction lowers its effective ionic radius, leaving less room for coordinating hydroxyl ions around the Al and reducing its coordination number from 6 to 4 (Cotton and Wilkinson, 1962, pp. 335, 342). The dominant aqueous complex now becomes $Al(OH)_4^-$. Within the transition interval the dominant aqueous complexes are in sequence $AlOH^{2+}$ and $Al(OH)_2^+$, and we have assumed that the coordination of Al in them is still 6-fold. The complex $Al(OH)_3^0$ appears to be negligible (May *et al.*, 1979).

The pH-dependent equilibria between each of the octahedrally coordinated species $[Al(H_2O)_6]^{3+}$, $[Al(OH)(H_2O)_5]^{2+}$, and $[Al(OH)_2(H_2O)_4]^+$ and the tetrahedrally coordinated species $[Al(OH)_4]^-$ can be written as

$$\begin{aligned} [Al(H_2O)_6]^{3+} + 4\,OH^- &= [Al(OH)_4]^- + 6\,H_2O, \\ [Al(OH)(H_2O)_5]^{2+} + 3\,OH^- &= [Al(OH)_4]^- + 5\,H_2O, \\ [Al(OH)_2(H_2O)_4]^+ + 2\,OH^- &= [Al(OH)_4]^- + 4\,H_2O \end{aligned} \quad (1)$$

[1] Present address: KRTA Ltd., P.O. Box 9806, Auckland, New Zealand.

Table 1. Equilibria and constants.

Equilibrium	log K 25°C	log K 100°C
$Al^{3+} + 4\,OH^- = Al(OH)_4^-$	33.84[1]	32.9[2]
$AlOH^{2+} + 3\,OH^- = Al(OH)_4^-$	24.79[1]	23.83[2]
$Al(OH)_2^+ + 2\,OH^- = Al(OH)_4^-$	15.99[1]	~15[3]
$H_2O = H^+ + OH^-$	−13.997[4]	−12.26[4]

[1] Values calculated from internally consistent data in May *et al.* (1979) and Coutourier *et al.* (1984).
[2] Values deduced by extrapolation of data in Coutourier *et al.* (1984).
[3] Estimated.
[4] Fisher and Barnes (1972).

Because the dissociation of the hydrated complexes on the left of these three equilibria to their respective non-hydrated complexes have equilibrium constants of unity at any temperature and pressure (obtained by appropriate choices of standard states, see Lewis *et al.*, 1961, p. 272), reactions (1) can be replaced respectively by those in Table 1, which also gives the log K values used here. The reactions in Table 1 can thus be used to describe both the speciation of aqueous Al and the equilibrium between octahedral and tetrahedral aqueous Al.

Disregarding for simplicity activity coefficients and combining the mass balance for Al, which is

$$m_{Al,tot} = \underset{\text{octahedral}}{m_{Al^{3+}} + m_{AlOH^{2+}} + m_{Al(OH)_2^+}} + \underset{\text{tetrahedral}}{m_{Al(OH)_4^-}}, \quad (2)$$

with the equilibrium conditions for the reactions in Table 1,

$$K_1 = m_{Al(OH)_4^-}\, a_{H^+}{}^4/K_w{}^4 m_{Al^{3+}},$$
$$K_2 = m_{Al(OH)_4^-}\, a_{H^+}{}^3/K_w{}^3 m_{AlOH^{2+}},$$
$$K_3 = m_{Al(OH)_4^-}\, a_{H^+}{}^2/K_w{}^2 m_{Al(OH)_2^+}, \quad (3)$$

one obtains

$$m_{Al^t(OH)_4^-}/m_{Al,tot} = [1 + (a_{H^+}{}^2/K_3K_w{}^2) + (a_{H^+}{}^3/K_2K_w{}^3) + (a_{H^+}{}^4/K_1K_w{}^4)]^{-1}, \quad (4)$$

where a and m represent activity and molality of the subscripted species, and K_w is the dissociation constant of water. Eq. (4) is plotted in Figure 1. The transition from predominantly octahedral to predominantly tetrahedral aqueous Al takes place over a narrow pH interval, namely about 5.5–6.5 at 25°C and 4–5 at 100°C. This narrow pH range is called below a threshold or a quasi-step function.

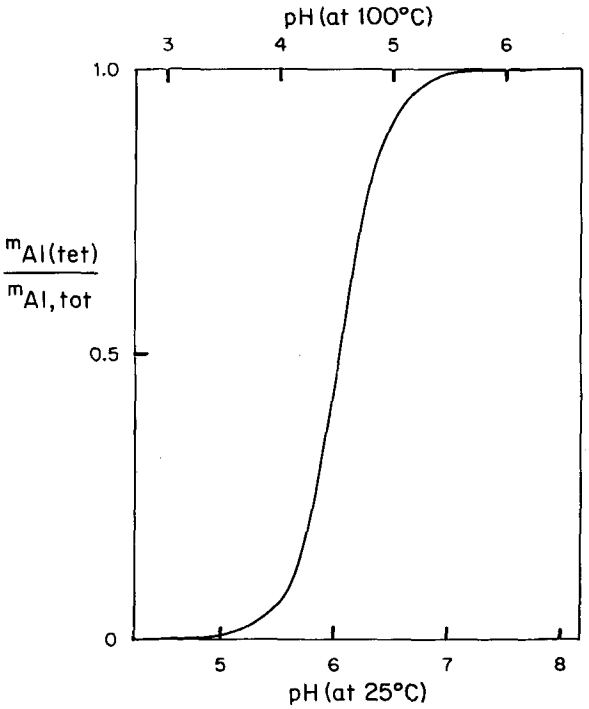

Figure 1. Predicted distribution of ratio of tetrahedrally coordinated Al to total tetrahedral plus octahedral Al in aqueous solutions at 25° and 100°C, based on Eq. (4) and data from May *et al.* (1979) and Coutourier *et al.* (1984). Note narrow pH range "threshold" over which aqueous Al goes from predominantly octahedral to predominantly tetrahedral coordination. This threshold pH decreases with increasing temperature.

DISSOLUTION OF TETRAHEDRAL ALUMINUM IN QUARTZ

By the mass-action law, crystals of a silicate growing from an aqueous solution should incorporate Al^t for Si. The rate and the extent of incorporation should be proportional to the aqueous concentration of Al^t (e.g., Weston and Schwarz, 1972, p. 6), itself a quasi-step function of the pH, as shown in Figure 1. As shown below for quartz, the mole fraction of Al^t taken up in solid solution depends also on aqueous variables other than the molality of tetrahedrally coordinated aqueous Al, and, of course, on the specific constraints of the structure of the mineral in question. The considerations in this section should apply also to other minerals (e.g., opal-CT, kaolinite, halloysite, and pyrophyllite) which accept only a small amount of Al^t.

The substitution of Al^{3+} for Si^{4+} in tetrahedral sites of quartz involves also the coupled incorporation of monovalent cations to balance charge (e.g., Deer *et al.*, 1966, p. 346; Smith and Steele, 1984). To describe these substitutions the components Si_4O_8 (= I) and $MAl^tSi_3O_8$ (= II) were chosen. (Si_4O_8 was chosen instead of SiO_2 as the pure silica component to equalize

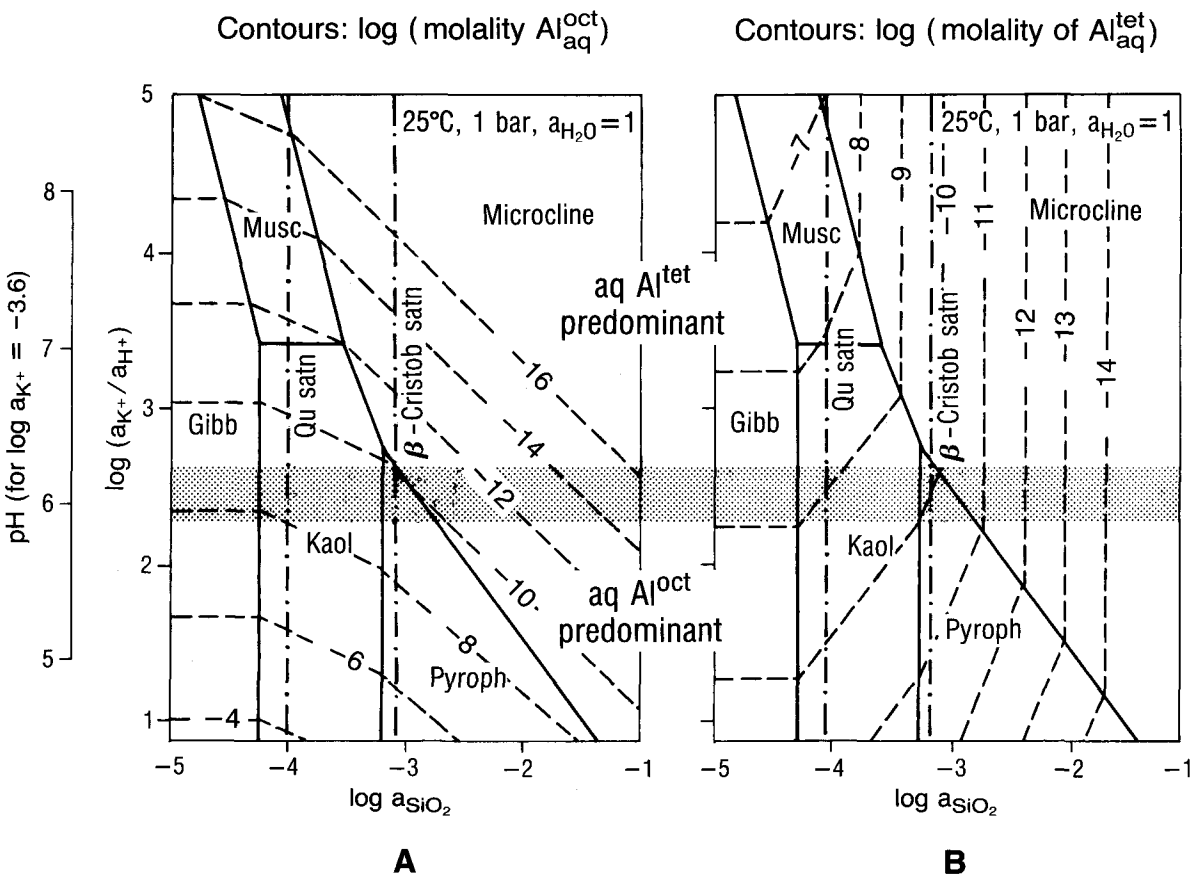

Figure 2. Relations among pH, aqueous-Al coordination, and Al coordination in minerals in the system K_2O-Al_2O_3-SiO_2-H_2O, at 25°C, 1 bar, activity of water = 1. Thermodynamic data are from Bowers *et al.* (1984). Stippled band is threshold from predominant octahedral Al (Al^o) to predominant tetrahedral Al (Al^t) in the aqueous solution, as taken from Figure 1. Note that threshold shifts downward for increasing temperature and upward for increasing aqueous K^+ concentration. pH scale shown at left and dashed contours of equilibrium log(molality) imposed by the system for aqueous octahedral Al (left) and aqueous tetrahedral Al (right) are for an arbitrary log(K^+ molality) = −3.6. Gibbsite proxies for other oxyhydroxides of Al; muscovite and pyrophyllite proxy for illite and smectite (Aagaard and Helgeson, 1984); kaolinite proxies for halloysite and other kaolin-group minerals; microcline proxies for K-zeolites. Note that kaolinite, halloysite, pyrophyllite, quartz, and opal-CT that crystallize *above* the aqueous Al^o/Al^t threshold should incorporate significant Al^t to degree permitted by each crystal structure and according to Eq. (7).

the numbers of oxygens in the two components, thus making their molar volumes similar. This choice avoided introducing a fictitious, large excess free energy.) Intracrystalline equilibrium is represented by

$$\underset{(I)}{Si_4O_8} + Al^t(OH)_{4,aq}^- + M_{aq}^+ = \underset{(II)}{MAl^tSi_3O_8} + SiO_{2,aq} + 2\,H_2O, \quad (5)$$

for which

$$K' = m_{SiO_2}x_{II}\lambda_{II}/m_{M^+}m_{Al(OH)_4^-}x_I\lambda_I, \quad (6)$$

where K' is the equilibrium constant for reaction (5), x is the mole fraction of components I (= Si_4O_8) or II (= $MAl^tSi_3O_8$), and λ is the activity coefficient of I or II in the silicate solid solution. For $M^+ = Na^+$, $K' = 10^{5.47}$ at 25°C (using data from Bowers *et al.*, 1984). Because quartz accepts only a very small mole fraction of component II (Deer *et al.*, 1966, p. 346), $x_I \approx 1$; and because the solvent of a very dilute solution obeys Raoult's law, $\lambda_I \approx 1$. Thus,

$$x_{II} = K'm_{M^+}m_{Al(OH)_4^-}/\lambda_{II}m_{SiO_2}, \quad (7)$$

which recovers the mass-action law statement given above and in addition yields an expression for the proportionality constant between x_{II} and the molality of $Al^t(OH)_4^-$.

As an illustration, aqueous $Al^t(OH)_4^-$ concentrations at equilibrium with pure phases in the system K_2O-Al_2O_3-SiO_2-H_2O are given by logarithmic contours in Figure 2b; $m_{Al^t(OH)_4^-}$ exponentially increases upward and to the left in pH-silica activity space. Figure 2a gives equilibrium contours of the log of the sum of all

aqueous octahedral species molalities (i.e., first three on the right of Eq. (2)) throughout the diagram. At any point

$$m_{\mathrm{Al,total}} = \begin{cases} m_{\mathrm{Al^o}} & \text{below the threshold} \\ m_{\mathrm{Al^{iv}(OH)_4^-}} & \text{above the threshold.} \end{cases}$$

(The pH scale in Figure 2 corresponds to the arbitrary choice log $m_{K^+} = -3.6$. As m_{K^+} increases, both the log m_{Al} contours and the pH scale shift upward with respect to the stability fields, which remain put.)

Eq. (7) approximately gives the mole fraction of component II (= $MAl^{t}Si_3O_8$) taken up by the quartz solid solution, with $m_{Al^{iv}(OH)_4^-}$ given by Eq. (4) and Figure 1. At low pHs (<threshold in Figure 1), x_{II} is low, because $m_{Al^{iv}(OH)_4^-}$ is low. At pHs > threshold, x_{II} becomes suddenly one or more orders of magnitude greater, because so does $m_{Al^{iv}(OH)_4^-}$. Note also that large amount of total dissolved Al and high monovalent cation concentration increase Al^{t} uptake by quartz, but high aqueous silica concentration reduces it and so does λ_{II}, which represents the structural constraints of the mineral to Al^{t} acceptance. Because solid solution of Al^{t} in minerals such as quartz, kaolinite, halloysite, and pyrophyllite is highly non-ideal (as required by the fact that it takes place only to a very limited extent), the activity coefficient, λ_{II}, of the $MAl^{t}Si_3O_8$ component in Eqs. (6) and (7) should be one or more orders of magnitude greater than unity, even for the excess-free-energy-minimizing choice of components made above.

Eq. (7) applies for the Al^o/Al^{t} pH threshold shown in Figure 1, but H^+ adsorption by crystal surfaces should introduce two modifications: (1) It should change the pH "seen" by the Al ions in the water boundary layer (perhaps a few tens of Ångstroms thick from the crystal surface), thus modifying the Al^o/Al^{t} ratio there. (2) It should also endow the crystal surface with an electrical charge, which, depending on the mineral and the specific crystal face involved (Parks, 1967), would favor or inhibit attachment of tetrahedral or octahedral aqueous Al to that face. This attachment contributes to crystal growth proper only if it takes place at kinks, but it would only change the activation barrier to crystal growth if it takes place on an atomically smooth crystal surface (e.g., see Chernov, 1984, pp. 104 ff. and his Figure 3.1). No attempt is made here to quantify these effects.

CRYSTAL MORPHOLOGY AND Al^{t}-FOR-Si SUBSTITUTION

The greater the degree of Al^{t}-for-Si substitution in halloysite, the more bent (usually around the *b* axis) become the 1:1 layers of this mineral (Bates, 1959, 1971; Radoslovich, 1963; Brindley, 1980, pp. 145, 158; Harvey, 1980, pp. 282–284; and Drever, 1982, Figure 4-4). In fact, for most halloysites the Al/Si atom ratio is greater than unity, implying the presence of some Al^{t}: of the many halloysite analyses in Deer *et al.* (1966), Weaver and Pollard (1973), and Newman and Brown (1987), only one (no. 2, p. 251, Deer *et al.*, 1966) has no Al^{t}. Coupled to this Al/Si > 1 ratio are the facts that many halloysites are tubular and that some Al is indeed tetrahedral. This latter evidence comes from nuclear magnetic resonance work by Komarneni *et al.* (1985) on a halloysite from Eureka, Utah. From its chemical analyses (nos. 15 and 17 in Table 70 of Weaver and Pollard, 1973, p. 151) we have calculated for this halloysite a structural formula that does contain Al^{t}.

These considerations suggest a genetic link between the composition of the aqueous solution (especially pH; also the concentrations of Al(total), monovalent cations, and silica) and the composition and morphology of halloysite crystals grown from it. The link takes place by means of solid solution of Al^{t} for Si, and it may well operate in other low-temperature silicates.

NATURAL EVIDENCE

The predictions made above regarding Al^{t} incorporation by low-temperature silicates and its relations to aqueous chemistry can be checked against the compositions of paired waters and authigenic silicates that coexist in nature, or which have reached equilibrium in hydrothermal experiments. Several water-mineral pairs from the literature are assessed and collected in Table 2 and plotted on the activity diagrams of Figures 3–5. All the waters plotted in the diagrams of Figures 3 and 5 have pHs greater than the octahedral/tetrahedral threshold in Figure 1, and, in agreement with the predictions above, the minerals coexisting with them (except one) are reported to contain some tetrahedral Al. The exception (Figure 3, water 'c') is from the northern end of Lake Chad. A saponite found in a vertisol there coexists with interstitial water that has a high pH, but the saponite nevertheless contains no Al^{t} (see Table 2). Two possible reasons for this discrepancy are: (1) Al was scavenged by the kaolinite coexisting with the saponite (Tardy *et al.*, 1974); and (2) the water's relatively high silica concentration (the largest for all waters plotted in Figure 3) would, according to Eqs. (7) or (8), depress the mole fraction of Al^{t} incorporated by the saponite.

The log $m_{Al^{iv}(OH)_4^-}$ value calculated here on the basis of equilibrium with Mg-montmorillonite for waters 6, 8, and 18 from Amboseli, Kenya (see Table 2 and figure 3; Stoessell and Hay, 1978) is about −8, which agrees well with the log $m_{Al,total}$ values measured analytically (which range from −6.7 to 7.7), if the formation of minor amounts of Al complexes with sulfate and fluoride is taken into account.

The water sample plotted in the diagram of Figure 4 has a pH < threshold, and the halloysite coexisting with it indeed contains no Al^{t}, also in agreement with

Table 2. Occurrences of coexisting pairs of waters and silicates, with aqueous activities and mineral structural formulae.[1]

	Locality													
	Bone Valley Fm., Florida[2]		Chad basin, Africa[2]			DSDP Site 323, South Pacific[2]		Amboseli, Kenya[2]			Ojo Caliente, Mexico[7]	Kettleman North Dome, Calif.			
Reference	(1)		(2, 3, 11)			(4, 5)		(6, 7)			(8)	(9, 10)			
Water no.[3]	[4]	(10)	a	b	c	650-m depth		(6)	(8)	(11)		88	41	30	26
pH	7.1	7.5	7.0	8.4 −3.5	8.1	7.7		8.15	8.30	7.90	3.5–3.7	8.61	8.55	8.18	8.50
log SiO_2	−3.15	−3.78	−3.33		−2.7	−3.90		−3.05	−3.00	−2.80	−2.67	−3.91	−3.60	−3.17	−4.09
log K^+/H^+	nd[9]	nd	3.04	13.43		4.00		5.10	4.50	4.38	0.04–0.24	4.81	5.22	5.72	5.03
log $Mg^{2+}/(H^+)^2$	11.38	11.73	10.56		11.62	13.51		12.70	13.05	12.65	1.9–2.3	12.31	12.58	11.92	11.58
log Al_{tot}	nd[9]	nd	nd	nd	nd	nd		−7.73	−6.68	−6.94	−4.22	nd	nd	nd	nd
Mineral[5]	montmoril[6]		nontr[4]	beidel[4]	sapon[4]	smect[6]	celad[4]	sepiol[4]		kerol[4]	halloys[6]	illites[4]			
Li	0.11														
Na	0.04				0.19	0.27		0.07		0.12	0.06	0.09	0.05	0.04	
K	0.11					0.15	0.89	0.04		0.03		0.28	0.65	0.79	0.73
Ca	0.19		0.22	0.133		0.13				0.04	0.01	0.01			
Fe^{2+}	0.01		1.77	0.50	0.16						0.01	0.03	0.04	0.01	0.02
Mg	0.65		0.21	0.26	1.90	0.37	0.76	1.90		2.99		0.16	0.05	0.11	0.20
Mn						0.37									
Al^o	2.43			1.327	0.51	1.08	0.36				3.62	1.82	1.94	1.82	1.78
Ti	0.06										0.14				
Fe^{3+}	0.57					1.34	0.88	0.03		0.01		0.18	0.04	0.07	0.11
Al^t	0.78		0.17	0.267	0.0	0.45	0.12	0.08		0.04		0.70	0.82	0.73	0.87
Si	7.2		3.83	3.733	4.0	3.55	3.88	2.94		3.91	4.12	3.30	3.18	3.27	3.13
O	18.08		10.00	10.00	10.00	6.96	10.00	7.5		10.09	10.00	10.00	10.00	10.00	10.00
OH	5.92		2.00	2.00	2.00	11.04	2.00	1.0		2.00	8.00	2.00	2.00	2.00	2.00
H_2O								3.07		2.62					

[1] See activity diagrams in Figures 3–5.

[2] See Figure 3.

[3] Activities and activity ratios given were obtained by calculation of distribution of aqueous species for Chad, Amboseli, and Kettleman water samples, but were taken as equal to the respective analytical molalities for all the other waters.

[4] Structural formula given in original reference.

[5] Authigenic mineral associated with water above; abbreviations correspond to montmorillonite, nontronite, beidellite, saponite, smectite, celadonite, sepiolite, kerolite, and halloysite.

[6] Structural formula calculated here from chemical analysis in original reference.

[7] See Figure 4.

[8] Each of the four authigenic illites given (see reference 10) is an average of all the (analyzed) illites associated with the corresponding interstitial water sample; the average Al^t values are shown in Figure 5 next to each corresponding water sample.

[9] nd = not determined.

(1) Altschuler *et al.* (1963); (2) Gac (1979); (3) Paquet (1969); (4) Kastner and Gieskes (1976); (5) Drever (1976); (6) Stoessell and Hay (1978); (7) Stoessell (1988); (8) Keller *et al.* (1971); (9) Merino (1975); (10) Merino and Ransom (1982); (11) Tardy *et al.* (1974).

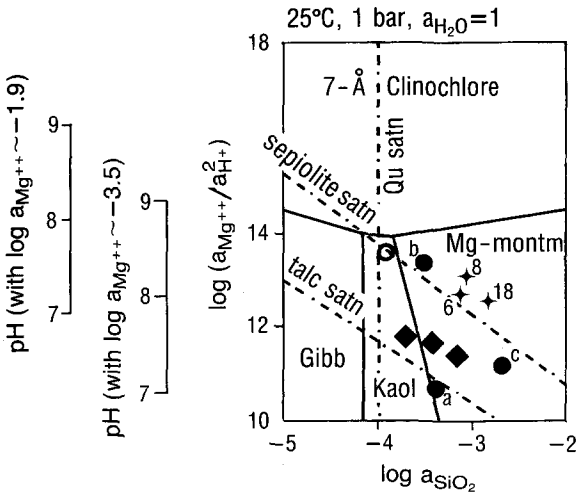

Figure 3. Activity diagram of log $Mg^{2+}/(H^+)^2$ vs. log(silica), showing pH and compositions of waters that coexist with tetrahedral Al (Al^t)-bearing phyllosilicates. All points representing waters fall well into field of predominant aqueous tetrahedral Al of Figure 2. Thus, coexisting silicates should also contain significant Al^t. All do, except saponite coexisting with water 'c', discussed in text. Compositions of waters and minerals are listed in Table 2. Position of pH scale at left depends on aqueous Mg^{2+} concentration of each water. Solid squares represent water samples coexisting with montmorillonite (Altschuler *et al.*, 1963). Solid circles a, b, and c represent water samples coexisting, respectively, with nontronite, beidellite, and saponite (Gac, 1979; Paquet, 1969). Open circle represents interstitial water coexisting with smectite and celadonite (Kastner and Gieskes, 1976; Drever, 1976). Stars represent water samples coexisting with sepiolite and kerolite (Stoessell and Hay, 1978; Stoessell, 1988).

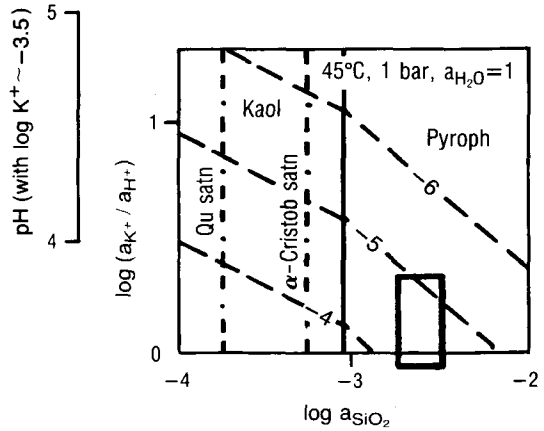

Figure 4. Activity diagram of log(K^+/H^+) vs. log(silica) at 45°C. Box represents hot spring water from Ojo Caliente, Michoacán, Mexico (Keller *et al.*, 1971) that coexists with halloysite. Water and halloysite compositions are in Table 2. Note that although most halloysites (see text) contain some tetrahedral Al, halloysite from Ojo Caliente contains none, as predicted from the fact that its coexisting water falls in the field of predominant aqueous octahedral Al, well below the threshold of Figures 1 and 2. Value of log(aqueous Al molality) of −4.3 to −5 predicted by diagram (contours are equilibrium log m_{Al^o} values) agrees well with analytical value of Table 2 reported by Keller *et al.* (1971).

our predictions. This occurrence is particularly significant because (see references above) halloysite usually contains some Al^t. The log m_{Al^o} of −5 to −4.5 predicted in Figure 4 for the Ojo Caliente hot water on the basis of equilibrium with the mineral phases agrees well with the analyzed log $m_{Al,total}$ of −4.22 reported by Keller *et al.* (1971), after allowing for the formation of minor amounts of Al complexes with ligands other than OH^-. This agreement is evidence of close approach to equilibrium between the halloysite and the water.

The four 100°C aqueous solutions from Kettleman North Dome plotted in Figure 5 have high pHs and coexist with Al^t-bearing diagenetic illite, in qualitative agreement with the prediction. Here, however, unlike for quartz, halloysite, kaolinite, and pyrophyllite, the amount of Al^t substituting for Si is not small; illite (as well as other micas, chlorites, feldspars, and zeolites) contains a major amount of Al^t as an essential constituent; all these minerals are further discussed in the next section.

We have found no references to natural or experimental pairs of well-analyzed waters and silica minerals with which to test the prediction (see Eq. (7)) that quartz (or opal-CT) that precipitates from aqueous solutions having pHs greater than the octahedral-to-tetrahedral Al threshold should incorporate significant Al^t, but that quartz (or opal-CT) that grows from aqueous solutions having a pH < threshold should not. Abundant analytical evidence indeed exists that silica minerals incorporate Al (plus a monovalent cation) and that the Al is in tetrahedral coordination (see Smith and Steele, 1984; Webb and Finlayson, 1987; and references therein).

INTERNAL EVIDENCE FROM ACTIVITY DIAGRAMS

In all the activity diagrams of log(cation/hydrogen) vs. log(silica) for K^+, Na^+, Ca^{2+}, Mg^{2+}, and Fe^{2+} in the systems cation oxide-Al_2O_3-SiO_2-H_2O (Bowers *et al.*, 1984), minerals having stability fields at low cation/hydrogen values (i.e., for any given cation concentration, at low pHs) ideally contain no Al^t (gibbsite and other aluminum oxides and oxyhydroxides, kaolinite and polymorphs, pyrophyllite). Minerals near the top of the diagrams, however, do contain Al^t, including muscovite, paragonite, illite, margarite, clinochlore, chamosite, lizardite, ordered and disordered K-feldspars, albite, anorthite, and zeolites. The addition of sulfate to the activity diagrams in Figures 2, 4, and 5 introduces alunite, $KAl_3(SO_4)_2(OH)_6$, the stability field for which lies in the lower left (i.e., low pH) region of the diagrams. This is where one would predict alunite to occur on the basis of the pH control proposed here

of the aqueous Al^t-to-Al(total) ratio, together with the fact that Al in alunite is octahedrally coordinated (Hendricks, 1937). Thus, the activity diagrams themselves, collectively, are evidence of the control of the Al^t content of minerals by the pH of the aqueous solution. Nevertheless, because the pH is not the only control, stability boundaries between minerals having different proportions of Al^t generally are not horizontal: increasing aqueous silica promotes the precipitation of minerals more and more siliceous, which indirectly means minerals having less and less potential room for Al^o. In other words, increasing silica activity causes the Al^o/Al(total) ratio of the mineral to decrease from 1 for gibbsite, to 2/3 for muscovite and paragonite, to 0 for feldspars and zeolites in the upper part of the diagrams. This left-to-right decrease causes the gibbsite-muscovite and muscovite-feldspar (or zeolite) boundaries to have negative slopes.

SUMMARY AND CONCLUSIONS

By the mass-action law aqueous solutions tend to introduce their species into the minerals that precipitate from them, to the extent allowed by each crystalline structure. In particular, low-temperature silicates take up tetrahedral Al in substitution for Si in proportion to the concentration of Al^t in the aqueous solution. Because the latter concentration turns out to be almost a step function of the pH (Figure 1), so does the mole fraction of Al^t incorporated by a low-temperature silicate. Furthermore, this mole fraction of Al^t is also proportional to the concentrations of aqueous monovalent cations and total dissolved Al, and inversely proportional to that of aqueous silica.

Presumably the uptake of $Al^t(OH)_4^-$ needs to overcome a lower activation barrier if it attaches to a tetrahedral site than if it attaches to an octahedral site in the growing crystal. On the other hand, crystal surface charge, which is positive (negative) for pH < (>) the isoelectric point, probably tends to increase the activation energy both for the attachment of aqueous octahedral Al^{3+} at pH < threshold and for that of aqueous tetrahedral $Al(OH)_4^-$ at pH > threshold. This applies particularly to silicates having an isoelectric point not far from the aqueous Al^o-to-Al^t threshold pH.

For halloysite, the Al^t-for-Si substitution causes bending of the layers (e.g., Drever, 1982, Figure 4-4). A genetic link emerges among the solution composition (especially its pH; also its $m_{Al(total)}$, m_{M^+}, and m_{SiO_2}), the detailed chemistry of halloysite (which commonly includes significant Al^t and coupled monovalent cations), and the morphology of halloysite crystals, typically tubular about the *b* axis. Similar links may operate in other minerals.

The predicted pH control of the Al^t content of a silicate is consistent with the distribution of mineral stability fields in activity diagrams. Also, the prediction is confirmed by comparing coexisting waters and phyllosilicates from weathering, hydrothermal, and diagenetic occurrences. In the two pairs for which the waters were analyzed for Al, its concentration is close to equilibrium with the solid phases. As an additional check on the predictions made here, it would be useful to determine the Al^t content of quartz overgrowths (or other low-temperature silica phases) precipitated from Al-bearing waters of known pH and composition; we have found no such data in the literature. Conversely, analytically determined amounts of Al^t in authigenic low-temperature silicates such as quartz, opal-CT, kaolinite, halloysite, and pyrophyllite could be used to infer pH at crystallization. Knowledge of mole fractions of Al^t in those minerals and of the aqueous concentrations of monovalent cations, total dissolved aluminum, and silica, would allow us to infer (by Eq. (7)) the activity coefficients of the Al^t-bearing component in the mineral solid solution.

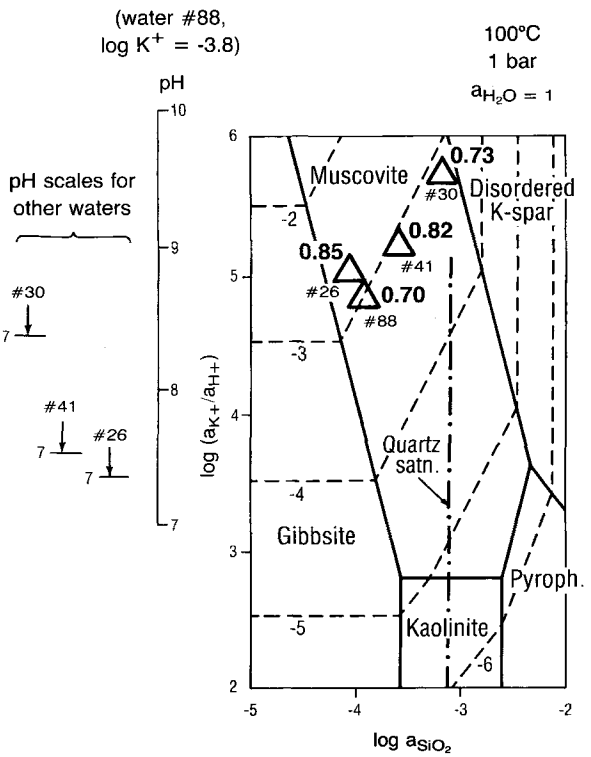

Figure 5. Activity diagram of $\log(K^+/H^+)$ vs. log(silica) at 100°C. Both dashed contours for log(molality of $Al(OH)_4^-$) and pH scale at left are constructed for $\log K^+ = -3.8$, which is the K^+ molality in Kettleman water sample 88. Triangles represent four interstitial aqueous solutions coexisting with diagenetic illites in Eocene McAdams sandstones in subsurface of Kettleman North Dome, California (Merino, 1975; Merino and Ransom, 1982). Triangle for water sample 88 falls on $\log m_{Al^t} = -3$ contour, shown. Next to each triangle is sample number of each interstitial water, and, in heavier type, the average Al^t per formula of diagenetic illites coexisting with that water sample.

ACKNOWLEDGMENTS

It is a pleasure to thank R. K. Stoessell, Yves Tardy, H. M. May, W. D. Keller, A. Hoch, A. Basu, B. F. Jones, D. Still, J. Tolen, B. Hill, and an anonymous reviewer for their help, suggestions, and constructive criticism. Acknowledgment is made to the Donors of the Petroleum Research Fund, administered by the American Chemical Society, for partial support of this research through grant 16636-AC2, and to the Department of Geology, Indiana University, for support.

REFERENCES

Aagaard, P. and Helgeson, H. C. (1984) Activity/composition relations among silicates and aqueous solutions: II. Chemical and thermodynamic consequences of ideal mixing of atoms on homological sites in montmorillonites, illites, and mixed-layer clays: *Clays & Clay Minerals* **31,** 207–217.

Altschuler, Z. S., Dwornik, E. J., and Kramer, H. (1963) Transformation of montmorillonite to kaolinite during weathering: *Science* **141,** 148–152.

Bates, T. F. (1959) Morphology and crystal chemistry of 1:1 layer lattice silicates: *Amer. Mineral.* **44,** 78–114.

Bates, T. F. (1971) The kaolin minerals: in *The Electron-Optical Investigation of Clays,* J. A. Gard, ed., Mineralogical Society, London, 109–148.

Bowers, T. S., Jackson, K. J., and Helgeson, H. C. (1984) *Equilibrium Activity Diagrams:* Springer-Verlag, Berlin, 397 pp.

Brindley, G. W. (1980) Order-disorder in clay mineral structures: in *Crystal Structures of Clay Minerals and their X-ray Identification,* G. W. Brindley and G. Brown, eds., Mineralogical Society, London, 125–195.

Chernov, A. A. (1984) *Modern Crystallography III. Crystal Growth:* Springer-Verlag, Berlin, 517 pp.

Cotton, F. A. and Wilkinson, G. (1962) *Advanced Inorganic Chemistry:* Wiley, New York, 959 pp.

Coutourier, Y., Michard, G., and Sarazin, G. (1984) Constantes de formation des complexes hydroxidés de l'aluminium en solution aqueuse de 20 à 70°C: *Geochim. Cosmochim. Acta* **48,** 649–659.

Deer, W. A., Howie, R. A., and Zussman, J. (1966) *Introduction to the Rock-forming Minerals:* Wiley, New York, 528 pp.

Drever, J. I. (1976) Chemical and mineralogical studies, site 323: in *Initial Reports of the Deep Sea Drilling Project, Vol. 35,* C. D. Hollister *et al.,* eds., U.S. Government Printing Office, Washington, D.C., 471–478.

Drever, J. I. (1982) *The Geochemistry of Natural Waters:* Prentice-Hall, Englewood Cliffs, N.J., 388 pp.

Fisher, J. R. and Barnes, H. L. (1972) The ion-product constant of water to 350°: *J. Phys. Chem.* **76,** 90–99.

Gac, J. Y. (1979) Géochimie du bassin du Lac Tchad: Bilan de l'altération, de l'érosion et de la sédimentation: Doctoral thesis, Univ. Louis Pasteur, Strasbourg, France, 249 pp.

Harvey, C. C. (1980) A study of the alteration products of acid volcanic rocks from northland, New Zealand: Ph.D. thesis, Indiana University, Bloomington, 322 pp.

Hem, J. D. and Robertson, C. E. (1967) Form and stability of aluminum hydroxide complexes in dilute solution: *U.S. Geol. Surv. Water-Supply Pap.* **1827A,** 55 pp.

Hendricks, S. B. (1937) The crystal structure of alunite and the jarosites: *Amer. Mineral.* **22,** 773–784.

de Jong, B. H. W. S., Schramm, C. M., and Parziale, V. E. (1983) Polymerization of silicate and aluminate tetrahedra in glasses, melts, and aqueous solutions. IV. Aluminum coordination in glasses and aqueous solutions and comments on the aluminum avoidance principle: *Geochim. Cosmochim. Acta* **47,** 1223–1236.

Kastner, M. and Gieskes, J. M. (1976) Interstitial water profiles and sites of diagenetic reactions, leg 35, DSDP, Bellingshousen abyssal plain: *Earth Plan. Sci. Lett.* **33,** 11–20.

Keller, W. D., Hanson, R. F., Huang, W. H., and Cervantes, A. (1971) Sequential active alteration of rhyolitic volcanic rock to endellite and precursor phase of it at a spring in Michoacân, Mexico: *Clays & Clay Minerals* **19,** 121–127.

Komarneni, S., Fyfe, C. A., and Kennedy, G. J. (1985) Order-disorder in 1:1 type clay minerals by solid state ^{27}Al and ^{29}Si magic-angle-spinning NMR spectroscopy: *Clay Miner.* **20,** 327–334.

Lewis, G. N., Randall, M., Pitzer, K. S., and Brewer, L. (1961) *Thermodynamics:* McGraw-Hill, New York, 723 pp.

May, H. M., Helmke, P. A., and Jackson, M. L. (1979) Gibbsite solubility and thermodynamic properties of hydroxy-aluminum ions in aqueous solution at 25°C: *Geochim. Cosmochim. Acta* **43,** 861–868.

Merino, E. (1975) Diagenesis in Tertiary sandstones from Kettleman North Dome, California. II. Interstitial solutions: Distribution of aqueous species at 100°C and chemical relation to the diagenetic mineralogy: *Geochim. Cosmochim. Acta* **39,** 1629–1645.

Merino, E. and Ransom, B. (1982) Free energies of formation of illite solid solutions and their compositional dependence: *Clays & Clay Minerals* **30,** 29–39.

Newman, A. C. D. and Brown, G. (1987) The chemical constitution of clays: in *Chemistry of Clays and Clay Minerals,* A. C. D. Newman, ed., Mineralogical Society, London, 1–128.

Parks, G. A. (1967) Aqueous surface chemistry of oxides and complex oxide minerals: in *Equilibrium Concepts in Natural Water Systems,* W. Stumm, ed., *Adv. Chem. Series* **67,** Amer. Chem. Soc., Washington, D.C., 121–160.

Paquet, H. (1969) Évolution géochimique des minéraux argileux dans les altérations et les sols des climats méditerranéens et tropicaux à saisons contrastées: *Mém. Serv. Carte Géol. Alsace Lorraine* **30,** 212 pp.

Radoslovich, E. W. (1963) The cell dimensions and symmetry of layer-lattice silicates. VI. Serpentine and kaolin morphology: *Amer. Mineral.* **48,** 368–378.

Smith, J. F. and Steele, I. M. (1984) Chemical substitution in silica polymorphs: *N. Jb. Miner. Mh.* **H.3,** 137–144.

Stoessell, R. K. (1988) 25°C and 1 atm dissolution experiments of sepiolite and kerolite: *Geochim. Cosmochim. Acta* **52,** 365–374.

Stoessell, R. K. and Hay, R. L. (1978) The geochemical origin of sepiolite and kerolite at Amboseli, Kenya: *Contrib. Mineral. Petrol.* **65,** 255–267.

Tardy, Y., Cheverry, C., and Fritz, B. (1974) Néoformation d'une argile magnésienne dans les dépressions interdunaires du Lac Tchad. Application aux domaines de stabilité des phyllosilicates alumineux, magnésiens et ferrifères. *C.R. Acad. Sci. Paris* **278** (Série D), 1999–2002.

Weaver, C. E. and Pollard, L. D. (1973) *The Chemistry of Clay Minerals:* Elsevier, Amsterdam, 213 pp.

Webb, J. A. and Finlayson, B. L. (1987) Incorporation of Al, Mg, and water in opal-A: Evidence from speleothems: *Amer. Mineral.* **72,** 1204–1210.

Weston, R. E. and Schwarz, H. A. (1972) *Chemical Kinetics:* Prentice-Hall, Englewood Cliffs, New Jersey, 274 pp.

(Received 30 July 1988; accepted 25 September 1988; Ms. 1768)